Journal of Fluids and Structures 17 (2003) 983–999

JOURNAL OF FLUIDS AND STRUCTURES

www.elsevier.nl/locate/jnlabr/yjfls

Aeroacoustoelasticity in state-space format using CHIEF regularization

M. Gennaretti*, U. Iemma

Department of Mechanical and Industrial Engineering, University Roma Tre 00146 Rome, Italy

Received 10 January 2002; accepted 14 March 2003

Abstract

This paper deals with aeroacoustoelastic modeling for analysis of the acoustic field inside an aircraft cabin. The aim is the identification of a state-space format for aeroacoustoelasticity equations applicable, for instance, for synthesis of an active control law devoted to cabin noise abatement. Specifically, attention is focused on the development of the aeroelastic operator, starting from a boundary integral equation method for the exterior compressible-aerodynamics solution. As is well known, in such a type of application of the boundary integral equation method, singularities occur in the algebraic equations resulting from discretization of the integral operator. Here, the discretized aerodynamic operator is regularized by using the CHIEF technique, that consists of augmenting the algebraic problem with homogeneous conditions at points in the interior domain (the cabin space, in our problem). Then, in order to obtain the state-space format model of the aeroacoustoelastic operator, the resulting trascendental aerodynamic transfer functions between structural Lagrangean variables and generalized aerodynamic forces are approximated through rational polynomials, and the additional aerodynamic states induced by their poles are included in the set of state-space variables.

1. Introduction

Modeling of aeroacoustoelastic phenomena concerning the fuselage of aircraft is the subject of the present paper. Specifically, our aim is the development of a state-space format model for the analysis of cabin noise in a conventional aircraft, with particular emphasis on the definition of coupling terms between fuselage elastic deformation and exterior aerodynamic flow (i.e., aeroelastic effects). Applications of an aeroacoustoelastic model of this type are found, for instance, in the synthesis of active control laws devoted to cabin noise abatement. Indeed, passenger comfort is an issue of primary interest in the design of modern turboprop midrange aircraft, and it can be significantly enhanced by combined implementation of active and passive noise abatement techniques.

Here, exterior aerodynamic loads are obtained by a boundary integral equation method (BIEM) for compressible potential flows that, for aeroelastic problems, seems to be the most efficient method of solution, from the computational point of view. Following this procedure, two types of problems arise in a fuselage aeroacoustoelastic formulation: the first is the presence of fictitious eigenfrequencies in the boundary integral aerodynamic operator, whereas the second stems from the presence of trascendental frequency terms in the aerodynamic transfer functions transforming structural displacements into aerodynamic loads (these trascendental terms are induced by the finiteness of speed of sound in compressible flows). Indeed, it may be shown that (Colton and Kress, 1983), a drawback in using a boundary-integral method in this type of external compressible-flow analysis is the presence of nonphysical (spurious) characteristic

*Corresponding author.
E-mail address: m.gennaretti@uniroma3.it (M. Gennaretti).

0889-9746/03/$ - see front matter
doi:10.1016/S0889-9746(03)00046-X

frequencies in the resulting boundary integral equation (extension to moving surfaces of the Kirchhoff–Helmholtz integral operator). In our case, where the exterior integral operator is of Neumann type, these spurious frequencies correspond to the eigenvalues of the Dirichlet interior problem (Colton and Kress, 1983), and the numerical solution of the integral operator can be completely destroyed by the presence of these fictitious eigenvalues (Schenck, 1968; Jones, 1974; Ursell, 1978; Amini, 1993). Moreover, taking into account the second problem arising in the aeroacoustoelastic formulation, it is easy to verify that the presence of trascendental terms in the aerodynamic transfer functions introduces an infinite number of eigenfrequencies in the acoustoelastic system and prevents the aeroacoustoelastic operator from being recast in time-domain state-space format (integro-differential terms would arise in its time-domain expression).

Here, developing the work presented by the authors in the past (Iemma et al., 1995; Iemma and Gennaretti, 1999; Gennaretti et al., 2000) and dealing with the two problems mentioned above, we address our analysis to the determination of a state-space format aeroacoustoelastic operator, including compressibility effects in solving the exterior aerodynamic flow solution. Problems generated by the presence of fictitious eigenfrequencies in the aerodynamic operator are overcome (in the frequency range of interest) by using the CHIEF regularization technique introduced by Schenck (1968). This technique consists of augmenting the set of equations of the discretized boundary integral operator with homogeneous condition equations at some points in the interior domain (cabin), followed by the application of a least-squares technique for the computation of unknowns (see Section 4). Next, once the regularized aerodynamic operator has been determined, following the approach suggested in Morino et al. (1995), and already applied in helicopter-rotor aeroelastic analysis in Gennaretti and Lisandrin (1998), the aerodynamic matrix (matrix in which we collect the whole set of aerodynamic transfer functions) will be approximated by a fraction-matrix expression, with coefficients evaluated through a least-squares approach (finite-state aerodynamic model, discussed in Appendix B). Indeed, although causing the introduction of a finite number of additional state variables, using this approximated aerodynamic matrix, it is possible to recast the aeroacoustoelasticity equations in state-space format (see Section 5).

Following the approach used by the authors in Iemma and Gennaretti (1999), the regularized finite-state aerodynamic operator is included in an acoustoelastic model for cylindrical fuselages, based on the Donnell–Mushtari differential model for elasticity of thin shells, combined with the wave equation problem for the interior pressure field. Both the fuselage elastic displacements and the interior pressure field are described in terms of linear combinations of orthogonal functions, and the Galërkin method is applied for determining the set of coupled time-differential equations governing the whole aeroacoustoelastic system.

Numerical results will be presented for showing the capability of the CHIEF approach to regularize the exterior compressible aerodynamic solution, and for validating the accuracy of the matrix-fraction approximation of the regularized aerodynamic matrix. Furthermore, in order to investigate the reliability of the introduced state-space aeroacoustoelastic model in cabin noise analysis, the noise field induced inside the cabin by some acoustic sources placed outside the fuselage is computed through the regularized aeroacoustoelastic model with the BIEM aerodynamic operator, and compared with that predicted by the approximated state-space aeroacoustoelastic model.

2. Aeroacoustoelastic model

A pressure perturbation generated from outside an aircraft cabin (e.g., by a propeller) is transmitted inside through elastic vibration of the fuselage structure. In this process, an important role is played by the unsteady aerodynamic loads acting on the fuselage, that arise due to (aeroelastic) interaction between elastic deformations of the fuselage shell and exterior flow. In this section, we briefly outline the formulation already used in the past by the authors (Iemma and Gennaretti, 1999) for modeling the transmission of sound from outside into the cabin, in order to focus the role of the unsteady aerodynamic operator, whose regularization and finite-state approximation will be analyzed later. This is an extension of the formulation introduced in Dowell et al. (1977), where the interior acoustics problem was analyzed in terms of a velocity potential function, and exterior aerodynamics effects were absent.

As discussed in details in Iemma and Gennaretti (1999), for the cabin space domain bounded by the fuselage, the pressure propagation problem may be described through a wave differential equation, forced at the domain contour by a term depending on the elastic motion of the fuselage structure, with Neumann-type homogeneous boundary conditions. Next, applying the Donnell–Mushtari theory for thin cylindrical shells, the structural dynamics of the simple-model fuselage considered here is described by a set of linear differential equations for the elastic displacements, with forcing terms arising from both exterior and interior pressure distributions, and shear diaphragm boundary conditions [see, e.g. Leissa (1973)]. Then, combining these two problems yields the integrated interior-acoustics/fuselage-vibration analysis, based on a coupled set of acoustoelastic differential equations forced by terms depending on the pressure distribution over the exterior of the fuselage skin. Here, the space integration of the problem is performed

by a spectral approach. Specifically, both the cabin pressure field and the elastic displacement of the fuselage skin are expressed in terms of linear combinations of orthogonal functions defined over the domain of interest [see, e.g. Iemma and Gennaretti (1999)], with the time-dependent coefficients representing the acoustoelastic Lagrangean variables of the problem. Next, the application of the Galërkin approach yields the following set of algebraic equations in the Laplace domain [see, e.g. Iemma and Gennaretti (1999)]:

$$[s^2\mathbf{M}^{el} + \mathbf{K}^{el}]\tilde{\mathbf{u}} = \mathbf{P}\tilde{\boldsymbol{\alpha}} + \tilde{\mathbf{f}}_{ext}, \tag{1}$$

$$[s^2\mathbf{M}^{ac} + \mathbf{K}^{ac}]\tilde{\boldsymbol{\alpha}} = s^2\mathbf{Q}\tilde{\mathbf{u}}, \tag{2}$$

where $\mathbf{u}$ and $\boldsymbol{\alpha}$ denote, respectively, structural and acoustic Lagrangean variables, $\mathbf{M}^{el}$, $\mathbf{K}^{el}$, $\mathbf{M}^{ac}$ and $\mathbf{K}^{ac}$ are mass and stiffness matrices of structural and acoustic problems, whereas $\mathbf{P}$ and $\mathbf{Q}$ are matrices arising due to the presence of the coupling terms mentioned above. In addition, in Eq. (1) $\mathbf{f}_{ext}$ denotes external loads acting on the fuselage given by combination of aeroelastic effects (fuselage-dynamics/exterior-flow interaction) and pressure perturbations. Therefore, we may write

$$\tilde{\mathbf{f}}_{ext} = \tilde{\mathbf{f}}_{ae} + \tilde{\mathbf{f}}_p = \check{\mathbf{E}}(s)\tilde{\mathbf{u}} + \tilde{\mathbf{f}}_p, \tag{3}$$

with $\check{\mathbf{E}}$ denoting the aerodynamic matrix transforming structural Lagrangean variables into generalized aerodynamic forces, and $\mathbf{f}_p$ denoting the generalized aerodynamic forces due to both incident perturbation pressure (e.g., that generated by a propeller) and pressure field scattered by the fuselage when considered as a rigid surface (rigidly scattered pressure).

Finally, denoting by

$$\mathbf{z} = \begin{Bmatrix} \mathbf{u} \\ \boldsymbol{\alpha} \end{Bmatrix}$$

the column matrix collecting the acoustoelastic Lagrangean variables, Eqs. (1) and (2) may be recast into the following aeroacoustoelastic system:

$$\left\{ s^2 \begin{bmatrix} \mathbf{M}^{el} & \mathbf{0} \\ -\mathbf{Q} & \mathbf{M}^{ac} \end{bmatrix} + \begin{bmatrix} \mathbf{K}^{el} & -\mathbf{P} \\ \mathbf{0} & \mathbf{K}^{ac} \end{bmatrix} - \begin{bmatrix} \check{\mathbf{E}}(s) & \mathbf{0} \\ \mathbf{0} & \mathbf{0} \end{bmatrix} \right\} \tilde{\mathbf{z}} = \begin{Bmatrix} \tilde{\mathbf{f}}_p \\ \mathbf{0} \end{Bmatrix}. \tag{4}$$

Note that, this expression cannot be written in state-space format, due to the presence of the aerodynamic matrix, $\check{\mathbf{E}}$, that is (as explained in the next section) a trascendental function of the frequency. Its rational-matrix approximation, suitable for recasting the aeroacoustoelastic system in state-space format, will be discussed in Section 5.

3. Potential-flow solution and aerodynamic matrix

The external unsteady loads acting on the fuselage are given by superposition of two pressure perturbations: namely, $\mathbf{f}_{ae}$ and $\mathbf{f}_p$ (Eq. (3)).

Forces $\mathbf{f}_p$ are due to incident and rigidly scattered fields induced by exterior acoustic sources, whereas forces $\mathbf{f}_{ae}$ are given by the perturbation field due to vibrations of fuselage shell (aeroelastic feedback). Here, the former is considered as a known external disturbance input to the aeroacoustoelastic system, whereas the attention is focused on the aeroelastic effects, that are modelled as explained in the following.

3.1. The aerodynamic matrix

Under the assumption of irrotational, compressible, subsonic flow, external aerodynamics is examined using a boundary integral equation formulation for the wave equation, in terms of a velocity potential function, φ, with Neumann-type impermeability boundary conditions, and the linearized Bernoulli theorem is applied for determining pressure distribution (Morino and Gennaretti, 1992). Then, observing that the most significant loads induced by aeroelastic effects are radial mode projections of the perturbation pressure due to radial elastic displacements, in the frequency domain these forces may be expressed as linear combinations of radial displacement Lagrangean variables, $\mathbf{w}$,

through an aerodynamic matrix $\mathbf{E}(s)$. Specifically, it is possible to show that, for

$$\mathbf{f}_{ae} = \left\{ \begin{array}{c} \mathbf{0} \\ \mathbf{0} \\ \mathbf{f}_{ae}^{(w)} \end{array} \right\},$$

with the first two null groups of rows representing the lack of significant projection of perturbation pressure onto fuselage membrane-displacement modes, one may write

$$\tilde{\mathbf{f}}_{ae}^{(w)} = \mathbf{E}(s)\tilde{\mathbf{w}} = \mathbf{E}_4\mathbf{E}_3(s)\mathbf{E}_2(s)\mathbf{E}_1(s)\tilde{\mathbf{w}}, \tag{5}$$

where matrix $\mathbf{E}_1(s)$ transforms radial Lagrangean variables into boundary conditions for the potential field, $\mathbf{E}_2(s)$ yields potential field solution through a boundary integral equation approach, $\mathbf{E}_3(s)$ transforms velocity potential field into pressure field over the body surface and, finally, $\mathbf{E}_4$ yields the generalized aerodynamic forces. Now, we examine the core of such procedure, i.e., the definition of matrix $\mathbf{E}_2(s)$ through discretization of the boundary integral equation formulation for the velocity potential (Morino and Gennaretti, 1992). Comparing with alternative methods for aerodynamic solution, the advantage in using this approach resides in the limited number of aerodynamic unknowns to deal with in evaluating $\mathbf{E}_2(s)$; whereas, as mentioned earlier, the drawback is that it introduces fictitious instabilities in the solution. This problem is analyzed (and regularized) in the next section whereas, for the sake of completeness, matrices $\mathbf{E}_1(s)$, $\mathbf{E}_3(s)$ and $\mathbf{E}_4$, are outlined in Appendix A.

3.2. *Non-regularized matrix* $\mathbf{E}_2$

For compressible, subsonic, potential flow about a nonlifting body (like the fuselage under examination here), it is possible to obtain the solution of the governing wave equation through the following frequency-domain boundary integral equation for the velocity potential, φ,

$$E(\vec{\mathbf{x}})\tilde{\varphi}(\vec{\mathbf{x}}) = \int_{\mathscr{S}_B} \left(G\frac{\partial\tilde{\varphi}}{\partial\hat{n}} - \tilde{\varphi}\frac{\partial G}{\partial\hat{n}} \right) \mathrm{e}^{-s\theta}\,\mathrm{d}\mathscr{S}(\vec{\mathbf{y}}) + \int_{\mathscr{S}_B} sG\tilde{\varphi}\frac{\partial\hat{\theta}}{\partial\hat{n}}\,\mathrm{e}^{-s\theta}\,\mathrm{d}\mathscr{S}(\vec{\mathbf{y}}), \tag{6}$$

where $\mathscr{S}_B$ represents the fuselage surface, $E(\vec{\mathbf{x}}) = 1$ for $\vec{\mathbf{x}}$ in the fluid domain, $E(\vec{\mathbf{x}}) = 1/2$ for $\vec{\mathbf{x}} \in \mathscr{S}_B$, and $E(\vec{\mathbf{x}}) = 0$ otherwise (Morino and Gennaretti, 1992). Furthermore,

$$G(\vec{\mathbf{x}}, \vec{\mathbf{y}}) = \frac{-1}{4\pi r_\beta}$$

is the unit source solution of the wave equation, where $r_\beta = \sqrt{[\vec{\mathbf{m}}_R \cdot (\vec{\mathbf{y}} - \vec{\mathbf{x}})]^2 + \beta^2 \|\vec{\mathbf{y}} - \vec{\mathbf{x}}\|^2}$, with $\vec{\mathbf{m}}_R = (-U_0/c)\vec{\mathbf{i}}$ denoting the Mach vector of the fuselage velocity, $\beta = \sqrt{1 - m_R^2}$, and $\theta = [r_\beta - \vec{\mathbf{m}}_R \cdot (\vec{\mathbf{y}} - \vec{\mathbf{x}})]/c\beta^2$ represents the time required by an acoustic perturbation to travel from $\vec{\mathbf{y}}$ to $\vec{\mathbf{x}}$ (acoustic time-delay). In addition, $\hat{\theta} = [r_\beta + \vec{\mathbf{m}}_R \cdot (\vec{\mathbf{y}} - \vec{\mathbf{x}})]/c\,\beta^2$, whereas $\vec{\mathbf{n}}$ denotes the fuselage outward unit normal, and

$$\frac{\partial(\cdot)}{\partial\hat{n}} = \frac{\partial(\cdot)}{\partial n} - \vec{\mathbf{m}}_R \cdot \vec{\mathbf{n}}\vec{\mathbf{m}}_R \cdot \vec{\nabla}(\cdot).$$

For the numerical solution of Eq. (6), a zeroth-order boundary element method (BEM) is used. To this aim, the body surface is divided into N_B quadrilateral elements (panels), where $\tilde{\varphi}$ and the normalwash, $\tilde{\chi}$, defined as

$$\tilde{\chi} = \frac{\partial\tilde{\varphi}}{\partial\hat{n}} \approx [1 - (\vec{\mathbf{m}}_R \cdot \vec{\mathbf{n}})^2]\frac{\partial\tilde{\varphi}}{\partial n} = \gamma\frac{\partial\tilde{\varphi}}{\partial n}$$

are assumed to be constant. The discretized expression of Eq. (6) satisfied at the centers of the panels (collocation method), may be written as

$$\frac{1}{2}\tilde{\varphi}_k = \sum_{j=1}^{N_B} (B_{kj}\tilde{\chi}_j + C_{kj}\tilde{\varphi}_j + sD_{kj}\tilde{\varphi}_j)\mathrm{e}^{-s\theta_{kj}} \tag{7}$$

with coefficients given by

$$B_{kj} = \int_{\mathscr{S}_{B_j}} G_k\,\mathrm{d}\mathscr{S}, \quad C_{kj} = -\int_{\mathscr{S}_{B_j}} \frac{\partial G_k}{\partial\hat{n}}\,\mathrm{d}\mathscr{S}, \quad D_{kj} = \int_{\mathscr{S}_{B_j}} G_k\frac{\partial\theta_k}{\partial\hat{n}}\,\mathrm{d}\mathscr{S},$$

where $\{\cdot\}_k = \{\cdot\}|_{\vec{\mathbf{x}}=\vec{\mathbf{x}}_k}$, and $\mathscr{S}_{B_j}$ denotes the surface of the jth panel. Next, denoting with $\boldsymbol{\varphi}$ the column matrix collecting values of potential at centers of panels, Eq. (7) may be recast in the form

$$\left[\frac{1}{2}\mathbf{I} - \mathbf{C}(s) - s\mathbf{D}(s)\right]\tilde{\boldsymbol{\varphi}} = \mathbf{B}(s)\tilde{\boldsymbol{\chi}}, \tag{8}$$

where $\mathbf{I}$ is the unit matrix and $\mathbf{B}$, $\mathbf{C}$, and $\mathbf{D}$ denote matrices whose entries are, respectively, $B_{kj}\mathrm{e}^{-s\theta_{kj}}$, $C_{kj}\mathrm{e}^{-s\theta_{kj}}$, and $D_{kj}\mathrm{e}^{-s\theta_{kj}}$. Finally, the (nonregularized) matrix $\mathbf{E}_2$ relating the potential vector, $\tilde{\boldsymbol{\varphi}}$, to the normalwash vector, $\tilde{\boldsymbol{\chi}}$, is given by

$$\mathbf{E}_2(s) = \left[\frac{1}{2}\mathbf{I} - \mathbf{C}(s) - s\,\mathbf{D}(s)\right]^{-1}\mathbf{B}(s). \tag{9}$$

In the next section, we examine those problems arising in evaluating such matrix, for the problem under consideration in this work.

4. CHIEF regularization of aerodynamic matrix

The aerodynamic transfer-function matrix introduced in the previous section is based on the potential field solution given by the boundary integral operator described in Eq. (6), that may be considered as an extension of the Kirchhoff–Helmholtz equation to arbitrary moving surfaces.

A drawback in following such an approach arises from the 'fictitious eigenvalue difficulty', consisting of the presence of eigenfrequencies in the boundary integral operator that yield a nonunique solution (Colton and Kress, 1983). Specifically, Eq. (6) relates the value of the velocity potential, φ, in the fluid domain to its distribution on the surface $\mathscr{S}_B$, with the value of normalwash, χ, on $\mathscr{S}_B$ known from Neumann-type impermeability boundary conditions: it is possible to show (Colton and Kress, 1983) that, for an integro-differential problem stated in this way, singularities appear at points in the Gauss plane corresponding to the resonant frequencies of the acoustic Dirichlet-boundary-value problem stated in the enclosure of $\mathscr{S}_B$. Then, when a numerical method is applied for solving Eq. (6), these spurious frequencies can completely destroy the solution. In our case, these singularities affect the evaluation of aerodynamic loads through the matrix $\mathbf{E}_2$ (Eq. (9)), and may deeply alter the aeroacoustoelastic response of the system.

Therefore, in order to overcome this difficulty, matrix $\mathbf{E}_2$ needs to be regularized. To this aim, we adopt the Combined Helmholtz Integral Equation Formulation (CHIEF) proposed by Schenck (1968). This method is based on the statement of an overdetermined set of algebraic equations for the unknown potential field, φ. Specifically, in applying the numerical solving procedure, it consists of adding N_c collocation points in the interior of the scattering surface (S_B) where, according to Eq. (6), we have $\tilde{\varphi} = 0$. The main advantage in using the CHIEF regularization method resides in the simplicity of its implementation, although particular attention must be paid in the space distribution of the interior collocation points: indeed, this approach is inefficient if they are not placed *sufficiently far* from the nodal lines of the acoustic natural modes of vibration of the cavity within the scattering surface.

Starting from Eq. (8), the resulting overdetermined system of equations has the following expression:

$$\mathbf{Y}\tilde{\boldsymbol{\varphi}} = \mathbf{Z}\,\tilde{\boldsymbol{\chi}}, \tag{10}$$

where the $[(N_B + N_c) \times N_B]$ matrices $\mathbf{Y}$ and $\mathbf{Z}$ are given by

$$\mathbf{Y} = \begin{bmatrix} (1/2)\mathbf{I} - \mathbf{C} - s\mathbf{D} \\ -\mathbf{C}^c - s\mathbf{D}^c \end{bmatrix} \quad \text{and} \quad \mathbf{Z} = \begin{bmatrix} \mathbf{B} \\ \mathbf{B}^c \end{bmatrix}, \tag{11}$$

with $\mathbf{C}^c, \mathbf{D}^c$ and $\mathbf{B}^c$ being $[N_c \times N_B]$ matrices collecting the influence coefficients relating potential and normalwash on the fuselage surface to the potential at the interior collocation points. Following the CHIEF method procedure, and defining $\tilde{\mathbf{b}} = \mathbf{Z}\,\tilde{\boldsymbol{\chi}}$, the solution, $\tilde{\varphi}$, of the above set of equations is determined as the vector that minimizes the quadratic form

$$\mathsf{J}(\tilde{\boldsymbol{\varphi}}) = \frac{1}{2}\left(\mathbf{Y}\tilde{\boldsymbol{\varphi}} - \tilde{\mathbf{b}}\right)^{*\mathrm{T}}(\mathbf{Y}\tilde{\boldsymbol{\varphi}} - \tilde{\mathbf{b}}), \tag{12}$$

and hence is given by

$$\tilde{\boldsymbol{\varphi}} = (\mathbf{Y}^{*\mathrm{T}}\mathbf{Y})^{-1}\mathbf{Y}^{*\mathrm{T}}\tilde{\mathbf{b}}. \tag{13}$$

Then, using the definition of vector $\tilde{\mathbf{b}}$, Eq. (13) yields the required regularized transfer matrix, $\mathbf{E}_2^c$, between the boundary condition $\tilde{\boldsymbol{\chi}}$ and the velocity potential $\tilde{\boldsymbol{\varphi}}$:

$$\mathbf{E}_2^c = (\mathbf{Y}^{*\mathrm{T}}\mathbf{Y})^{-1}\mathbf{Y}^{*\mathrm{T}}\mathbf{Z}. \tag{14}$$

The above $[N_B \times N_B]$ matrix is that introduced in Eq. (5) in order to determine the regularized aerodynamic transfer function, $\mathbf{E}$, between radial elastic displacements and generalized aerodynamic forces.

Note that, the presence of time-delayed terms in Eq. (6) and in Eq. (7) as well, is responsible for the trascendental dependence on the frequency of both matrices $\mathbf{E}_2$ and $\mathbf{E}$. They appear for the finiteness of speed of sound in compressible flows and describe a peculiar feature of the physical phenomenon under consideration, that has a considerable impact on the aeroacoustoelastic behavior of the system in that, at each instant, it influences the distribution of pressure perturbation over the vibrating shell.

5. Aeroacoustoelasticity in state-space format

The presence of the aerodynamic matrix in the aeroacoustoelastic operator makes it impossible to recast its original form in state-space format (and, at the same time, introduces an infinite number of eigenfrequencies), due to the trascendental expression of its entries. Hence, in order to achieve our goal (and, consequently, limit the number of system eigenfrequencies), now we introduce a suitable approximating expression for the aerodynamic matrix.

First, observe that (see Section 3 and Appendix B), whatever the model used for the prediction of the aerodynamic loads, the asymptotic behavior of the aerodynamic transfer functions is quadratic, as the frequency tends to infinity. Furthermore, time-delay terms occurring in matrix $\mathbf{E}_2^c$, suggest the presence of some poles in the expressions used for approximating these transfer functions. Therefore, following the formulation introduced by Morino et al. (1995), the expression of the approximated aerodynamic matrix that we adopt is (see Appendix B)

$$\mathbf{E}(s) \approx s^2\mathbf{A}_2 + s\mathbf{A}_1 + \mathbf{A}_0 + \mathbf{H}[s\mathbf{I} - \mathbf{G}]^{-1}\mathbf{F}, \tag{15}$$

where $\mathbf{A}_m$, $\mathbf{H}$, $\mathbf{G}$ and $\mathbf{F}$ are real and fully populated matrices. They are determined by a least-squares approximation technique applied along the imaginary axis, for minimizing differences with the computed values of the exact aerodynamic matrix (see Appendix B for details).

Now, we are ready to recast Eq. (4) in state-space format for aeroacoustoelastic analysis. Observe that, combining Eq. (5) with Eq. (15), the generalized forces due to aeroelastic effects may be expressed in the following approximated form:

$$\tilde{\mathbf{f}}_{ae}^{(w)} = \mathbf{E}(s)\tilde{\mathbf{w}} = (s^2\mathbf{A}_2 + s\mathbf{A}_1 + \mathbf{A}_0)\tilde{\mathbf{w}} + \mathbf{H}\tilde{\mathbf{r}}, \tag{16}$$

with

$$(s\mathbf{I} - \mathbf{G})\tilde{\mathbf{r}} = \mathbf{F}\tilde{\mathbf{w}}, \tag{17}$$

where $\mathbf{r}$ is a column matrix of new additional variables, whose dynamics is described by the poles introduced in the approximation procedure (the number of the additional variables is equal to the number of poles in the matrix-fraction approximation expression) and are a consequence of flow memory of past structural states due to time-delay terms in the velocity potential solution. Next, combining Eq. (4) with Eqs. (16) and (17) yields the following set of coupled equations for structural and acoustic Lagrangean variables, together with the additional variables introduced above:

$$(s^2\mathbf{M} + s\mathbf{D} + \mathbf{K})\tilde{\mathbf{z}} + \check{\mathbf{K}}\tilde{\mathbf{r}} = \tilde{\mathbf{p}}, \tag{18}$$

$$(s\mathbf{I} - \mathbf{G})\tilde{\mathbf{r}} - \check{\mathbf{F}}\tilde{\mathbf{z}} = \mathbf{0}, \tag{19}$$

where

$$\mathbf{M} = \begin{bmatrix} \mathbf{M}^{el} - \check{\mathbf{A}}_2 & \mathbf{0} \\ -\mathbf{Q} & \mathbf{M}^{ac} \end{bmatrix}, \quad \mathbf{D} = \begin{bmatrix} -\check{\mathbf{A}}_1 & \mathbf{0} \\ \mathbf{0} & \mathbf{0} \end{bmatrix}, \quad \mathbf{K} = \begin{bmatrix} \mathbf{K}^{el} - \check{\mathbf{A}}_0 & -\mathbf{P} \\ \mathbf{0} & \mathbf{K}^{ac} \end{bmatrix}, \quad \check{\mathbf{K}} = \begin{bmatrix} -\check{\mathbf{H}} \\ \mathbf{0} \end{bmatrix}, \quad \check{\mathbf{F}} = \begin{bmatrix} \bar{\mathbf{F}}, & \mathbf{0} \end{bmatrix},$$

and

$$\tilde{\mathbf{p}} = \begin{Bmatrix} \tilde{\mathbf{f}}_p \\ \mathbf{0} \end{Bmatrix},$$

whereas the matrices that describe aerodynamic effects are defined as (the first two groups of rows being related to membrane aerodynamic loads, and the first two groups of columns being related to membrane displacements),

$$\check{\mathbf{A}}_j = \begin{bmatrix} \mathbf{0} & \mathbf{0} & \mathbf{0} \\ \mathbf{0} & \mathbf{0} & \mathbf{0} \\ \mathbf{0} & \mathbf{0} & \mathbf{A}_j \end{bmatrix}, \quad \check{\mathbf{H}} = \begin{bmatrix} \mathbf{0} \\ \mathbf{0} \\ \mathbf{H} \end{bmatrix}, \quad \bar{\mathbf{F}} = [\mathbf{0}, \quad \mathbf{0}, \quad \mathbf{F}],$$

i.e., such that (see Eq. (3))

$$\tilde{\mathbf{f}}_{ae} = (s^2\check{\mathbf{A}}_2 + s\check{\mathbf{A}}_1 + \check{\mathbf{A}}_0)\tilde{\mathbf{u}} + \check{\mathbf{H}}\tilde{\mathbf{r}},$$

with

$$(s\mathbf{I} - \mathbf{G})\tilde{\mathbf{r}} = \bar{\mathbf{F}}\tilde{\mathbf{u}}.$$

Finally, transforming Eqs. (18) and (19) into time-domain, and defining the following column matrix of the augmented aeroacoustoelastic state variables

$$\mathbf{x} = \begin{Bmatrix} \dot{\mathbf{z}} \\ \mathbf{z} \\ \mathbf{r} \end{Bmatrix},$$

we obtain the following state-space format for the aeroacoustoelastic governing equations:

$$\dot{\mathbf{x}} = \mathbf{A}\,\mathbf{x} + \mathbf{f},$$

with

$$\mathbf{A} = \begin{bmatrix} -\mathbf{M}^{-1}\mathbf{D} & -\mathbf{M}^{-1}\mathbf{K} & -\mathbf{M}^{-1}\check{\mathbf{K}} \\ \mathbf{I} & \mathbf{0} & \mathbf{0} \\ \mathbf{0} & \check{\mathbf{F}} & \mathbf{G} \end{bmatrix}, \text{ and } \mathbf{f} = \begin{Bmatrix} \mathbf{M}^{-1}\mathbf{p} \\ \mathbf{0} \\ \mathbf{0} \end{Bmatrix}.$$

6. Numerical results

In this section, we show some numerical results obtained with the aeroacoustoelastic formulation presented above. The configuration used for the numerical validation refers to a general aviation aircraft. The fuselage is assumed to be a 12 mm-thickness cylindrical shell made of aluminum, that for the sake of aerodynamic analysis is closed at both ends by two emispherical domes (they do not vibrate under the action of unsteady loads, but ensure smoothness of streamlines). The length of the fuselage is $L = 7$ m, its radius is $r = 1$ m, and, for all the results presented, the flight speed is that corresponding to Mach number $M_\infty = 0.32$, and to a sea-level dynamic pressure equal to $q_D = 7300$ Pa. The analysis has been performed for the frequency range $f \leqslant 300$ Hz, which represents a reasonable limit for the class of aircraft under consideration (we assume the aircraft driven by a proprotor that rotates at an angular speed of about 600 rpm).

First, we present a comparison between the (nonregularized) $\mathbf{E}_2$ matrix and the (regularized) $\mathbf{E}_2^c$ matrix obtained from the application of the CHIEF technique (see Sections 2 and 4). As mentioned in Section 4, the CHIEF regularization technique is highly influenced by the choice of the additional collocation points. As a first step, a convergence analysis on the number of CHIEF collocation points has been performed, including up to 20 additional points inside the cabin. We have located an increasing number of points on a fuselage section positioned in a low-nodal-density region for the acoustic modes ($x/L = 0.05$ from the nose), in order to follow the criterion mentioned in Section 4 about CHIEF effectiveness. The convergence-analysis results about CHIEF regularization effects are presented in Figs. 1 and 2 for two elements of the matrix $\mathbf{E}_2$ (corresponding, respectively, to a fuselage-nose point and a middle-fuselage point) that have values differing for two order of magnitude. Specifically, we have computed the CHIEF solution for 2, 6, and 12 CHIEF points and the results show that, regardless of the magnitude of the matrix element, the regularization effect improves continuously with increasing number of points. Note that the range examined is about between 150 and 250 Hz, since it includes a high number of fictitious eigenvalues. A similar convergence behavior is observed in Figs. 3 and 4 where, fixing four points per section, we considered up to five sections along the fuselage length (again, taking care in locating them in low-nodal-density regions for the acoustic modes). However, comparing Fig. 1 with Fig. 3, and Fig. 2 with Fig. 4, it appears that using 12 points distributed over three sections has a better regularization effect than using the same number of points on a single section. In Figs. 5 and 6 the nonregularized solution is compared with that obtained using 20 points distributed over five sections, which represents the most satisfactory solution in the frequency

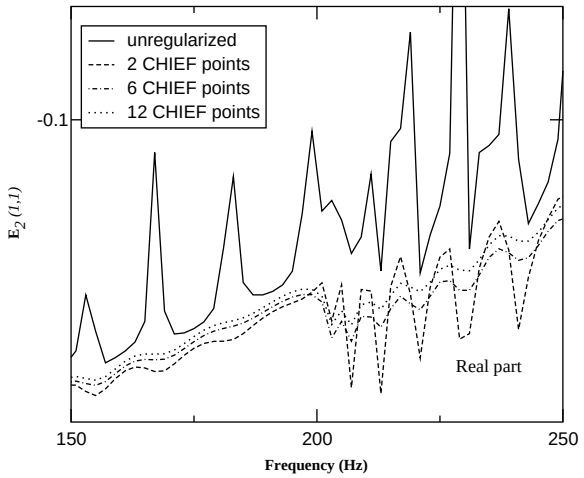

Fig. 1. Regularization of matrix $\mathbf{E}_2$. Convergence of the real part of entry $\mathbf{E}_2(1,1)$ for an increasing number of CHIEF points distributed on the $x/L = 0.05$ transverse section.

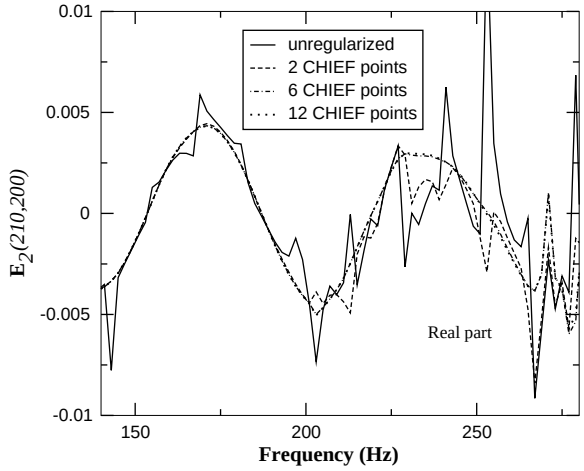

Fig. 2. Regularization of matrix $\mathbf{E}_2$. Convergence of the real part of entry $\mathbf{E}_2(210,200)$ for an increasing number of CHIEF points distributed on the $x/L = 0.05$ transverse section.

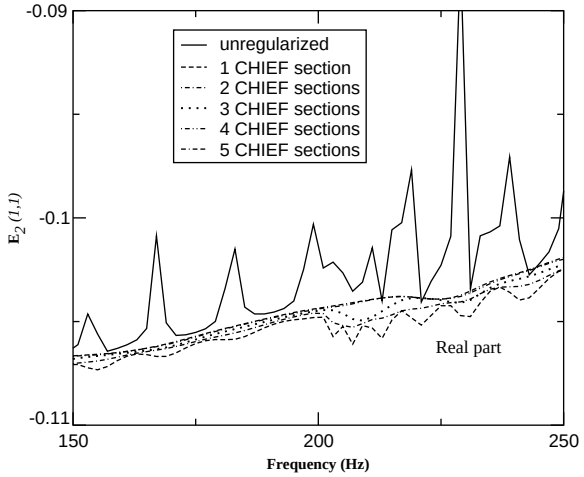

Fig. 3. Regularization of matrix $\mathbf{E}_2$. Convergence of the real part of entry $\mathbf{E}_2(1,1)$ for an increasing number of transverse sections.

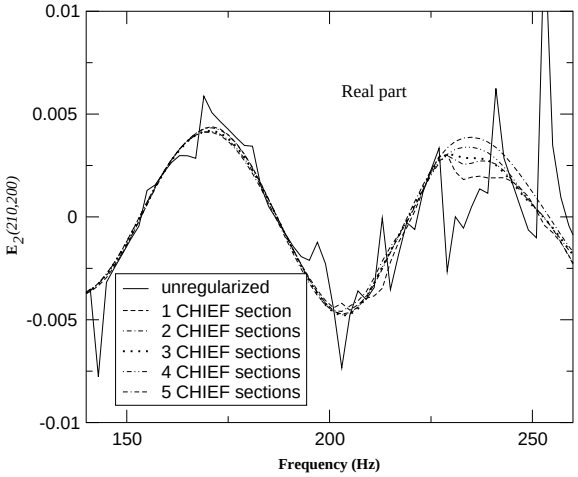

Fig. 4. Regularization of matrix $\mathbf{E}_2$. Convergence of the real part of entry $\mathbf{E}_2(210, 200)$ for an increasing number of transverse sections.

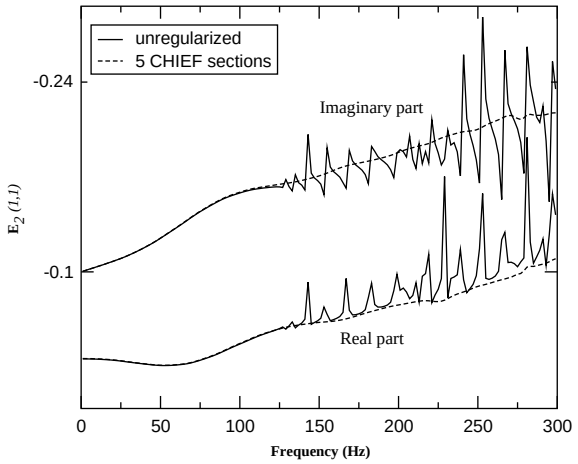

Fig. 5. Regularization of matrix $\mathbf{E}_2$. Spectrum of the real and imaginary part of entry $\mathbf{E}_2(1, 1)$ (regularized matrix obtained with 20 CHIEF points equally distributed on five transverse sections).

range of interest for the present analysis. It is worth noting that, the inclusion of these additional collocation points does not affect appreciably the computational cost of the solution.

Next, we approach the problem of approximating the aerodynamic matrix $\mathbf{E}$. Indeed, as explained in Section 5, the effect of the rational-matrix approximation of the aerodynamic operator is two-fold: (i) introducing a finite number of additional state-space variables, it makes it possible to determine the time-domain description of aerodynamic loads without presence of convolution integrals and, (ii), in the frequency domain, it reduces to a finite value the number of system eigenfrequencies. In order to limit the number of additional states (and of system eigenfrequencies, as well) in the rational-matrix-approximation procedure, it is convenient to request a high level of accuracy in the shortest frequency range compatible with the analysis purposes. Hence, it is necessary to identify the frequency range where aerodynamics plays the most important role in the aeroacoustoelastic response. To this end, using 10 natural modes of vibrations for the description of each component of the structural displacement, we have analyzed the frequency spectra of fuselage radial displacement and of interior acoustic pressure induced by a given incident pressure distribution (see Fig. 7 and Table 1 for details on distribution and intensity of incident pressure and location of observation points).

The results that have been obtained are presented, respectively, in Figs. 8 and 9, where the solid lines represent responses without influence of exterior aerodynamics, whereas dashed lines depict responses with regularized-aerodynamics effects. It can be noted that: (i) as expected, exterior aerodynamics cannot be neglected in the whole

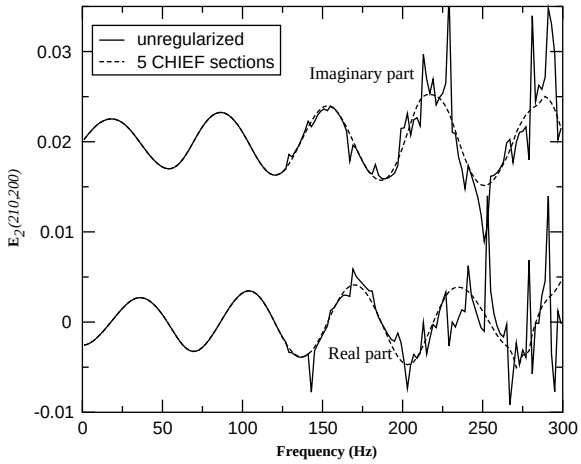

Fig. 6. Regularization of matrix $\mathbf{E}_2$. Spectrum of the real and imaginary part of entry $\mathbf{E}_2(210, 200)$ (regularized matrix obtained with 20 CHIEF points equally distributed on five transverse sections).

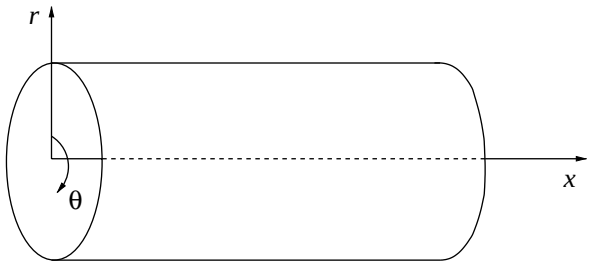

Fig. 7. Sketch of fuselage reference axes.

Table 1
Source-observer parameters

	x/L	r/R	θ	$\|\|p_{\text{inc}}\|\|/q_D$
Source point # 1	0.37	1	0	0.14
Source point # 2	0.21	1	0	0.10
Source point # 3	0.51	1	0	0.13
Source point # 4	0.37	1	$\pi/10$	0.08
Source point # 5	0.37	1	$-\pi/10$	0.08
Pressure observer	0.14	0.8	$\pi/15$	—
Shell-displacement observer	0.14	1	$\pi/15$	—

frequency range examined and (ii) the elastic response (directly affected by exterior aerodynamics) is much more relevant in the low-frequency range (see dashed line in Fig. 8). Therefore, in the finite-state approximation process, we have requested a high level of accuracy in the range of frequency up to 100 Hz, limiting the procedure to the capture of the mean value of the spectrum in the remaining part of the frequency range considered. Specifically, the aerodynamic matrix, $\mathbf{E}$, of dimensions $[10 \times 10]$ in our problem, has been evaluated by the regularized BEM solver at 75 frequencies uniformly distributed in the range $[0, 100]$ Hz, and at 25 frequencies uniformly distributed in the range $[100, 200]$ Hz. These data have been considered as the aerodynamic sampled data in the approximation procedure, in which we have assumed $M = 7$ (see Eq. (B.1)), therefore introducing 70 additional aerodynamic states. Then, following the methodology described in Appendix B, after elimination of the unstable poles, we have iteratively obtained the final approximating expression that includes 47 (stable) additional states (it is worth noting that, an extension of the high-accuracy frequency region would increase this number of additional states).

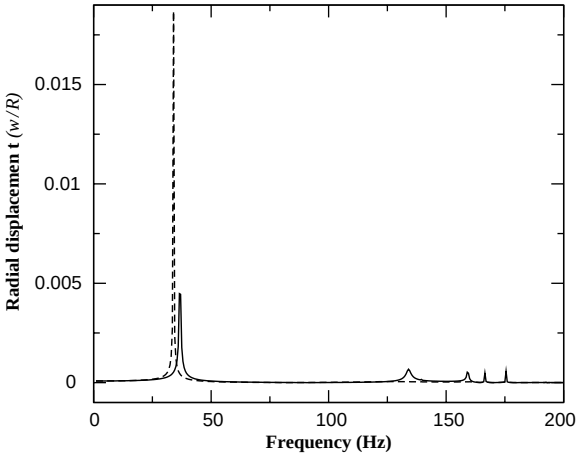

Fig. 8. Influence of exterior aerodynamics on the spectrum of radial displacement. ——, without exterior aerodynamics; - - -, with exterior aerodynamics.

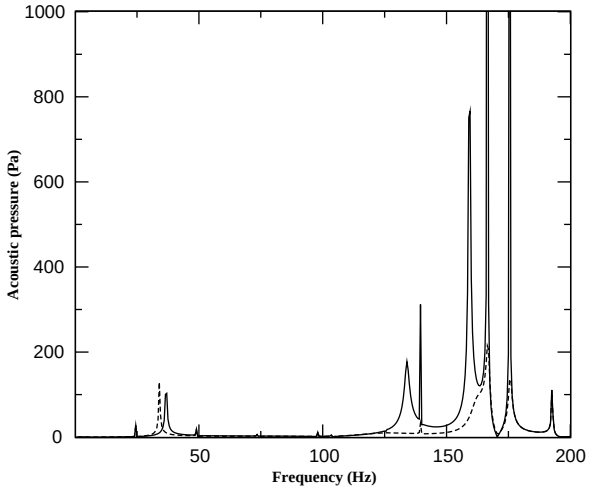

Fig. 9. Influence of exterior aerodynamics on the interior acoustic pressure.——, without exterior aerodynamics; - - -, with exterior aerodynamics.

For three of the most significant entries of the aerodynamic matrix, Figs. 10–12 show the comparison between BEM-evaluated transfer functions (solid lines) and the their rational matrix approximations (dashed lines), showing that the accuracy requested is obtained. Note that, as observed in Appendix B, the high number of additional states required in our analysis is due to the high number of transfer functions (i.e., the number of entries of matrix **E**) that are approximated simultaneously (therefore involving the same set of poles).

Finally, in Fig. 13 the spectrum of the interior acoustic pressure obtained with the approximated aerodynamic matrix is compared with that given by using the regularized, but not approximated, aerodynamic operator. The agreement is excellent in the whole range examined, and in particular at the higher frequencies, where a lower level of accuracy was requested in the approximation procedure. The only exception stands in the second peak of the response where, although having perfectly captured its position in the spectrum, the finite-state aerodynamics overestimates its amplitude. This can be explained by observing that, despite the overall satifactory accuracy of the finite-state model shown in Figs. 10–12, some local discrepancies are detectable. In particular, Figs. 14 and 15 show that, in the vicinity of the second peak of the acoustic response in Fig. 13, the approximated imaginary part is in good agreement with the exact BEM solution, whereas the approximated real part greatly overpredicts the BEM solution. This fact, combined with the great influence on the structural response of the inclusion of the aerodynamic operator (see Fig. 8, in the frequency range under examination), causes the overprediction of the amplitude of the second peak. It is worth noting

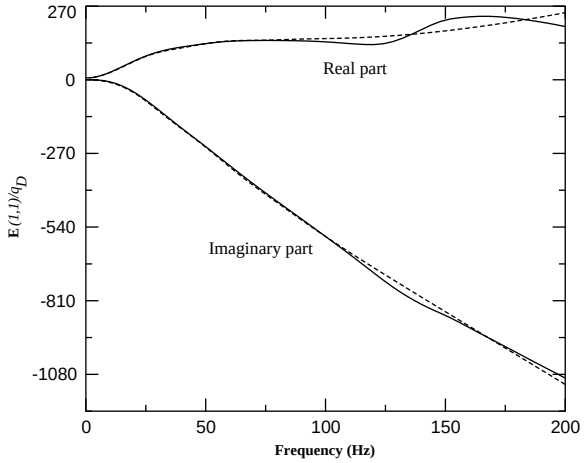

Fig. 10. Matrix-fraction approximation of matrix **E**. Spectrum of real and imaginary part of entry $\mathbf{E}(1,1)$ divided by the dynamic pressure, q_D. ——, BEM aerodynamics; - - -, finite-state aerodynamics.

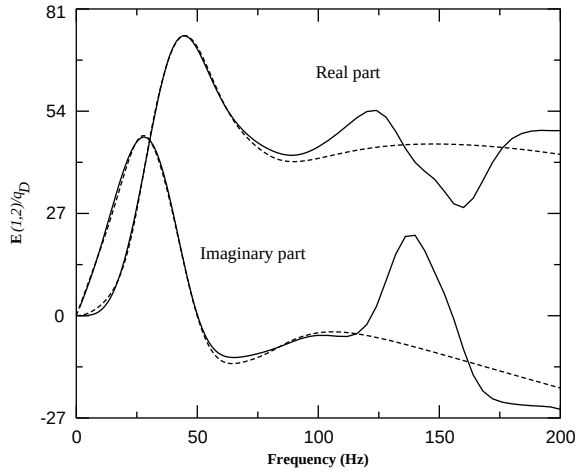

Fig. 11. Matrix-fraction approximation of matrix **E**. Spectrum of real and imaginary part of entry $\mathbf{E}(1,2)$ divided by the dynamic pressure, q_D. ——-, BEM aerodynamics; - - -, finite-state aerodynamics.

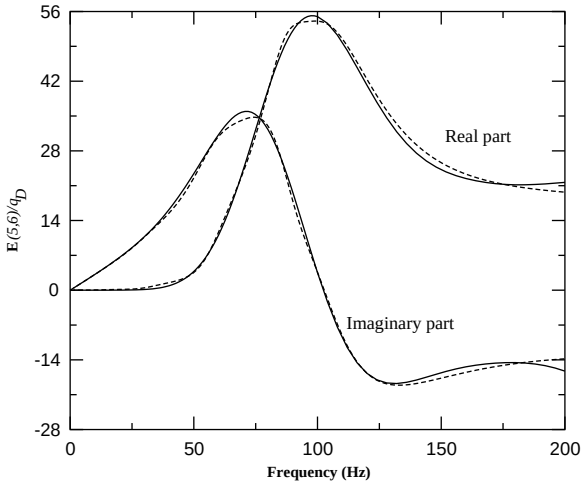

Fig. 12. Matrix-fraction approximation of matrix **E**. Spectrum of real and imaginary part of entry $\mathbf{E}(5,6)$ divided by the dynamic pressure, q_D. ——, BEM aerodynamics; - - -, finite-state aerodynamics.

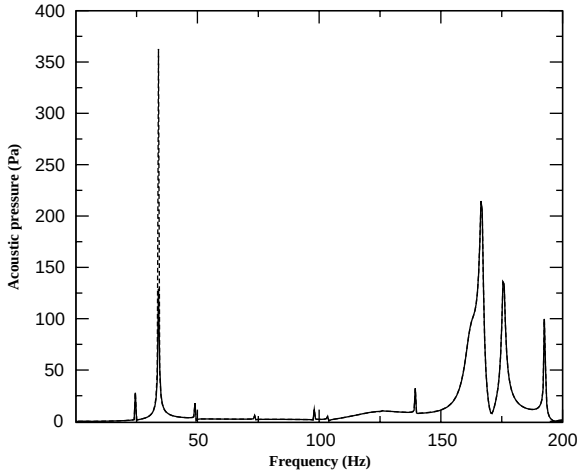

Fig. 13. Comparison between interior pressure spectrum obtained using exact (BEM) aerodynamics and that obtained using finite-state aerodynamics. ——, BEM aerodynamics; - - -, finite-state aerodynamics.

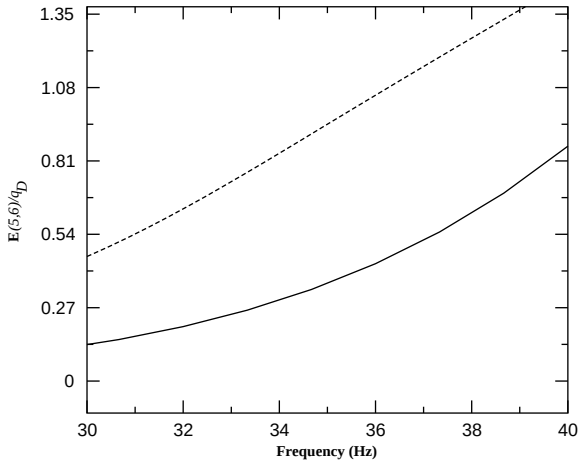

Fig. 14. Matrix-fraction approximation of matrix **E**. Spectrum of real part of entry $\mathbf{E}(5,6)$ divided by the dynamic pressure, q_D, in a frequency range around the second peak in Fig. 13. ——, BEM aerodynamics; - - -, finite-state aerodynamics.

that, observing Fig. 13, it is evident that this sensitivity to the aerodynamic operator approximation does not occur at high frequencies. Indeed, Figs. 8, 9, and 13 reveal that, although it is important, the inclusion of aerodynamic damping effects, even via a very rough approximation, yields a very good prediction of the acoustic response.

7. Conclusions

For aircraft fuselages traveling within a compressible flow, we have derived a state-space format aeroacoustoelastic model, based on a boundary integral method for the solution of the external aerodynamics. Two main issues have been investigated, in the frequency range of interest for cabin noise induced by aircraft propellers: the first one is the regularization of the discretized boundary integral operator for the external flow solution via CHIEF technique, whereas the second one is the finite-state approximation of the aerodynamic matrix via matrix-fraction approximation. A convergence analysis on the number of CHIEF points included in the computation has shown that a satisfactorily regularized aerodynamic solution can be achieved with about 20 CHIEF points, whose inclusion causes a negligible additional computational cost. Then, the matrix-fraction approximation procedure has been applied to the regularized aerodynamic transfer function, yielding a quite accurate analytical description of the aerodynamic operator, with the

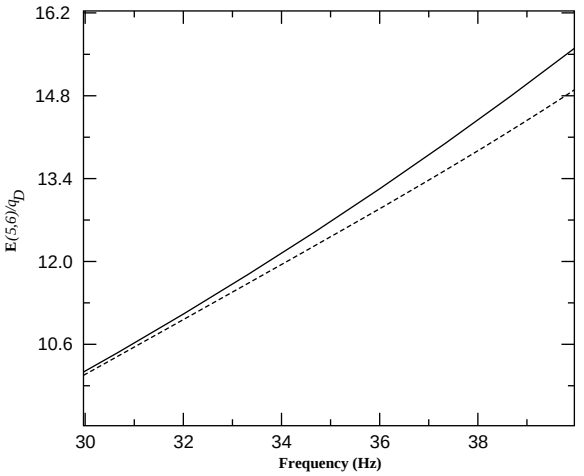

Fig. 15. Matrix-fraction approximation of matrix $\mathbf{E}$. Spectrum of imaginary part of entry $\mathbf{E}(5,6)$ divided by the dynamic pressure, q_D, in a frequency range around the second peak in Fig. 13. ——, BEM aerodynamics; - - -, finite-state aerodynamics.

inclusion of 47 additional states (poles) in the analysis. Finally, the aeroacoustoelastic operator has been recast in a state-space format, and numerical results have shown its capability of predicting the interior acoustic field induced by an arbitrary distribution of external sources.

On the basis of the numerical results discussed above, it seems that the finite-state approximation strategy proposed in this paper, that consists of a multi-level accuracy approximation in the frequency range of interest (high accuracy at low frequencies and viceversa), is very efficient in the aeroacoustoelastic modelling, where it has been shown that a rough estimate of the aerodynamic damping at high frequencies (allowing a reduction of added aerodynamic states) yields satisfactory predictions of the acoustic response. Therefore, the technique presented in this paper appears to be a reliable tool for including exterior unsteady aerodynamic effects in a state-space aeroacoustoelastic model, that can be conveniently applied, for instance, in synthesis of active noise-control laws.

Appendix A. Matrices $\mathbf{E}_1$, $\mathbf{E}_3, \mathbf{E}_4$ in the aerodynamic matrix

Here, we outline the definition of matrices $\mathbf{E}_1, \mathbf{E}_3$ and $\mathbf{E}_4$ that, combined with (regularized) matrix $\mathbf{E}_2^c$, compose the aerodynamic transfer-function matrix, $\mathbf{E}$, that introduces aeroelastic effects in the acoustoelastic system. Although their derivation is not a peculiar aspect of the methodology presented in this paper, their definition is helpful in addressing the problem of finite-state modelling of the aerodynamic matrix, especially in the choice of approximating expression (see Section 5).

A.1. Matrix $\mathbf{E}_1$

Once the potential flow solution matrix, $\mathbf{E}_2$, has been defined (Section 3), it is possible to observe that source of perturbation for the exterior potential field is the normalwash distribution (proportional to the normal component of flow velocity) over the fuselage surface. Then, under small disturbance assumption, we determine the (linear) contribution to normalwash due to (radial) elastic motion of the fuselage shell. This is given in terms of matrix $\mathbf{E}_1$, collecting the corresponding transfer functions.

For the total normalwash we have

$$\frac{\hat{\chi}}{\gamma} = \vec{\mathbf{v}} \cdot \vec{\mathbf{n}} = (U_0\vec{\mathbf{i}} + \vec{\mathbf{v}}_{el}) \cdot (\vec{\mathbf{n}}_0 + \vec{\mathbf{n}}') = \frac{1}{\gamma}(\chi_0 + \chi), \tag{A.1}$$

where $-U_0\vec{\mathbf{i}}$ is the rigid-body fuselage velocity, $\vec{\mathbf{v}}_{el}$ denotes the velocity of the elastic deformation, $\vec{\mathbf{n}}_0$ denotes the fuselage external normal in the undeformed configuration, $\vec{\mathbf{n}}'$ represents the variation of the fuselage normal due to the elastic displacement, and $\chi_0 = U_0 \cdot \vec{\mathbf{n}}_0 z$ is the steady state flow normal component. Expressing the radial displacement as $w(\vec{\mathbf{x}}, t)\sum_{n=1}^{N} w_n(t)\Phi_n(\vec{\mathbf{x}})$ (being $\Phi_n(\vec{\mathbf{x}})$ the chosen radial modal functions), combining with Eq. (A.1), and neglecting higher order terms in the perturbation variables, w_n, we obtain the following frequency-domain expression for the

perturbation normalwash on the fuselage

$$\tilde{\chi} = s\sum_{n=1}^{N} \tilde{w}_n \, \Phi_n - U_0 \vec{\mathbf{i}} \cdot \vec{\mathbf{n}}'_L, \tag{A.2}$$

where $\vec{\mathbf{n}}'_L = \vec{\mathbf{n}}'_L(\tilde{w}_n)$ is the linear approximation of $\vec{\mathbf{n}}'$, expressed in terms of the radial structural Lagrangean variables. Finally, denoting with $\mathbf{w}$ the column matrix collecting Lagrangean variables of the radial displacement, w_n, and with $\boldsymbol{\chi}$ the column matrix collecting values of normalwash at collocation points over the fuselage, Eq. (A.2) may be recast in the following matrix form:

$$\tilde{\boldsymbol{\chi}} = \mathbf{E}_1(s)\tilde{\mathbf{w}}.$$

A.2. Matrix $\mathbf{E}_3$

The linearized Bernoulli theorem is the starting point for the determination of the transfer function matrix between potential field and pressure over the fuselage surface. In a frame of reference connected with a body having velocity $-U_0\vec{\mathbf{i}}$, it has the form $\partial\varphi/\partial t + U_0\partial\varphi/\partial \mathsf{x} + p/\rho = p_\infty/\rho$. Then, in the frequency domain the pressure perturbation, p', is given by

$$\tilde{p}' = -\rho\left[s\tilde{\varphi} + U_0\frac{\partial\tilde{\varphi}}{\partial \mathsf{x}}\right].$$

Discretizing $\partial\tilde{\varphi}/\partial\mathsf{x}$ by a finite-difference scheme, this equation may be recast as

$$\tilde{\mathbf{p}} = \mathbf{E}_3(s)\tilde{\boldsymbol{\varphi}},$$

where $\mathbf{E}_3(s)$ is the resulting matrix operator, and $\mathbf{p}$ is the column matrix of the perturbation pressure values at collocation points on the fuselage surface.

A.3. Matrix $\mathbf{E}_4$

Finally, the generalized forces related to the shape functions of the fuselage radial elastic deformation, Φ_n, are given by

$$\tilde{f}_n^{(w)} = -\int_{\mathsf{S}_B} \tilde{p}'\Phi_n \, \mathrm{d}\mathscr{S} \approx -\sum_{j=1}^{N_B} \tilde{p}'_j \int_{\mathsf{S}_{B_j}} \Phi_n \, \mathrm{d}\mathscr{S},$$

and hence, in matrix notation,

$$\tilde{\mathbf{f}}_{ae}^{(w)} = \mathbf{E}_4\tilde{\mathbf{p}}.$$

Appendix B. Matrix-fraction approximation

The procedure that has been applied for approximating the aerodynamic matrix stems from two observations: the first is that, whatever the model used for the prediction of the aerodynamic loads, the asymptotic behavior of the aerodynamic transfer functions is quadratic, and the second is that the presence of time-delay terms in the boundary integral operator for potential flow solution suggests the inclusion of poles in the approximating expression. Then, these two aspects are fulfilled by an approximating matrix-fraction expression of the following type for the aerodynamic matrix:

$$\mathbf{E}(s) \approx \hat{\mathbf{E}}(s) = s^2\hat{\mathbf{A}}_2 + s\hat{\mathbf{A}}_1 + \hat{\mathbf{A}}_0 + \left[\sum_{m=0}^{M} \mathbf{D}_m s^m\right]^{-1}\left[\sum_{m=0}^{M-1} \mathbf{R}_m s^m\right], \tag{B.1}$$

that coincide with that examined by Morino et al. (1995). Matrices $\hat{\mathbf{A}}_m$, $\mathbf{D}_m$ and $\mathbf{R}_m$ are real and fully populated (except for $\mathbf{D}_M$ that is chosen to be a unit matrix). They are determined by a least-squares approximation technique along the imaginary axis, that requires the satisfaction of the following condition:

$$\varepsilon^2 = \sum_j w_j \, \mathtt{Tr}[\mathbf{Z}^{*\mathrm{T}}(s_j)\mathbf{Z}(s_j)]|_{s_j=\mathrm{i}k_j} = \min, \tag{B.2}$$

where $\mathrm{i} = \sqrt{-1}$, w_j denotes a suitable set of weights, and

$$\mathbf{Z}(s) := \left[\sum_{m=0}^{M} \mathbf{D}_m s^m\right][s^2\hat{\mathbf{A}}_2 + s\hat{\mathbf{A}}_1 + \hat{\mathbf{A}}_0 - \mathbf{E}(s)] + \sum_{m=0}^{M-1} \mathbf{R}_m s^m$$

is a measure of the error $(\mathbf{E} - \hat{\mathbf{E}})$.

Finally, in order to use the matrix-fraction approximation of the aerodynamic matrix for recasting the aeroacoustoelastic problem of Eq. (4) in a state-space format, it is convenient to rewrite Eq. (B.1) in the following equivalent form

$$\mathbf{E}(s) \approx s^2\hat{\mathbf{A}}_2 + s\hat{\mathbf{A}}_1 + \hat{\mathbf{A}}_0 + \hat{\mathbf{H}}[s\mathbf{I} - \hat{\mathbf{G}}]^{-1}\hat{\mathbf{F}}, \tag{B.3}$$

where

$$\hat{\mathbf{H}} = [\mathbf{I}, \quad \mathbf{0}, \quad \cdots \quad \mathbf{0}, \quad \mathbf{0}], \quad \hat{\mathbf{F}} = \begin{bmatrix} \mathbf{R}_{M-1} \\ \mathbf{R}_{M-2} \\ \cdot \\ \cdot \\ \mathbf{R}_1 \\ \mathbf{R}_0 \end{bmatrix},$$

$$\text{and} \quad \hat{\mathbf{G}} = \begin{bmatrix} -\mathbf{D}_{M-1} & \mathbf{I} & \mathbf{0} & \ldots & \mathbf{0} \\ -\mathbf{D}_{M-2} & \mathbf{0} & \mathbf{I} & \ldots & \mathbf{0} \\ \cdot & \cdot & & & \cdot \\ \cdot & \cdot & & & \cdot \\ -\mathbf{D}_1 & \mathbf{0} & \mathbf{0} & \ldots & \mathbf{I} \\ -\mathbf{D}_0 & \mathbf{0} & \mathbf{0} & \mathbf{0} & \mathbf{0} \end{bmatrix},$$

with each submatrix having the same dimensions of matrix $\mathbf{E}$ [see Morino et al. (1995), for details]. Note that the accuracy of the approximation depends upon the number, M, of matrices used in the matrix-fraction term in Eq. (B.1). The appropriate value of M depends upon the characteristics and number of functions to be approximated: the more wavy is their behavior in the frequency domain, the higher is the value of M required for an accurate approximation, and therefore the higher is the number of poles included in the approximate expression. In our case, these functions have a quite regular behavior in the frequency domain, and the value of M required for an acceptable approximation is relatively small (4 or 5, depending on the accuracy requested); nonetheless, a high number of poles (eigenvalues of the matrix $\hat{\mathbf{G}}$) are present in Eq. (B.3), due to the very high number of functions to be approximated (equal to the square of the number of structural modes included in the analysis, i.e., of the order of hundreds for our problem).

Unfortunately, if a high number of poles is introduced, some of them could be found to be unstable, i.e., they could have real part greater than zero: these are spurious poles which are introduced by the interpolation procedure, and are not physically acceptable (if the input structural variables have limited amplitudes, aerodynamic forces have limited amplitudes, as well). In order to overcome this problem, the iterative procedure suggested by Morino et al. (1995) is adopted. This consists of: (i) diagonalization (or block-diagonalization) of $\hat{\mathbf{G}}$, (ii) truncation of the unstable poles (the matrix $\hat{\mathbf{G}}$ is modified into a smaller matrix $\mathbf{G}$), and (iii) application of an optimal fit iterative procedure to determine new matrices $\mathbf{A}_2$, $\mathbf{A}_1$, $\mathbf{A}_0$, $\mathbf{F}$, and $\mathbf{H}$ that replace, respectively, $\hat{\mathbf{A}}_2$, $\hat{\mathbf{A}}_1$, $\hat{\mathbf{A}}_0$, $\hat{\mathbf{F}}$, and $\hat{\mathbf{H}}$ (whereas $\mathbf{G}$ remains unchanged throughout the iteration). Hence, the matrix-fraction finite-state approximation assuring a good and stable fit of $\mathbf{E}(s)$ has the final form

$$\mathbf{E}(s) \approx s^2\mathbf{A}_2 + s\,\mathbf{A}_1 + \mathbf{A}_0 + \mathbf{H}[s\mathbf{I} - \mathbf{G}]^{-1}\mathbf{F}.$$

Note that, for fixed-wing aeroelastic applications, other finite–state reduction methods are currently available. Among these, the methods of Roger (1977) and Karpel (1982) are the most widely adopted. A detailed discussion of the relationship among these two approaches and that presented in this appendix can be found in Morino et al. (1995). However, here it is worth pointing out that, Karpel's method directly starts from an approximating expression of the type of that in Eq. (B.3). The effect of this choice is two-fold: first, the dimensions of matrix $\hat{\mathbf{G}}$ may be set arbitrarily in dependence of the number of additional states that are presumed to be necessary and, second, the solution of the least-squares problem for the identification of the coefficients in Eq. (B.3) requires the use of an iterative technique. On the other hand, in our approach we start from the approximating expression in Eq. (B.1), whose coefficients are determined by solving the linear algebraic equation resulting from the satisfaction of the condition described in Eq. (B.2) and then,

expession (B.3) is obtained by simply recasting the one in Eq. (B.1). Hence, in this case, no iteration is needed for determining the coefficients of the approximating expression, but the number of the additional states is forced to be M-times the number of the generalized forces described by the aerodynamic matrix and, if this number overestimates the number of the additional states required by problem, unstable poles arise and the iterative procedure described above has to be applied for their elimination. Therefore, Karpel's and our approaches are very similar, the main difference standing in the a priori choice of number of additional states in Karpel's one, that in ours is replaced by a self-fitting procedure.

Finally, as already noted by Karpel (1992) and further outlined in Morino et al. (1995), we mention that Roger's method can be considered as a particular case of the Karpel approach. In particular, for the same number of additional states, the latter may (or may not) include a higher number of degrees of freedom in the approximation procedure [i.e., coefficients in expression (B.3)] and therefore, although causing a more complex solution of the least-squares problem, it is expected to yield a more accurate finitestate model.

References

Amini, S., 1993. Boundary integral solution of the exterior Helmholtz problem. AIAA Paper 95-042.

Colton, D., Kress, R., 1983. Integral Equation Methods in Scattering Theory. Wiley, New York.

Dowell, E.H., Gorman III, G.F., Smith, D.A., 1977. Acoustoelasticity: general theory, acoustic natural modes and forced response to sinusoidal excitation, including comparisons with experiment. Journal of Sound and Vibration 52, 519–542.

Gennaretti, M., Lisandrin, P., 1998. Flap-lag rotor dynamics and aeroelastic stability using finite-state aerodynamics. 24th European Rotorcraft Forum, Marseilles, France.

Gennaretti, M., Iemma, U., Corbelli, A., 2000. Analysis of interior noise in a tiltrotor fuselage. Seventh International Congress on Sound and Vibration, Garmish-Partenkirchen, Germany.

Iemma, U., Gennaretti, M., 1999. Integrated aeroacoustoelastic modeling for the analysis of the propeller-driven cabin noise. AIAA Paper 99-1919.

Iemma, U., Morino, L., Trainelli, L., 1995. Internal noise generated by sources external to an elastic shell. First AIAA/CEAS Aeroacoustics Conference, Münich, Germany.

Jones, D.S., 1974. Integral equations for the exterior acoustic problem. Quarterly Journal of Mechanics and Applied Mathematics 27, 129–142.

Karpel, M., 1982. Design for the active flutter suppresion and gust alleviation using state-space aeroelastic modeling. Journal of Aircraft 19, 221–227.

Karpel, M., 1992. Size-reduction techniques for the determination of efficient aeroservoelastic model. Control and Dynamics Systems 54, 263–295.

Leissa, A.W., 1973. Vibration of Shells. NASA SP-288.

Morino, L., Gennaretti, M., 1992. Boundary integral equations methods for aerodynamics. In: Atluri, S.N. (Ed.), Computational Nonlinear Mechanics in Aerospace Engineering. Vol. 146, AIAA Progress in Aeronautics and Astronautics, Washington, DC.

Morino, L., Mastroddi, F., De Troia, R., Ghiringhelli, G.L., Mantegazza, P., 1995. Matrix fraction approach for finite-state aerodynamic modeling. American Institute of Aeronautics and Astronautics (AIAA) Journal 33, 703–711.

Roger, K.L., 1977. Airplane math modeling methods for active control design. AGARD-CP 228.

Schenck, H.A., 1968. Improved integral formulation for acoustic radiation problems. Journal of the Acoustical Society of America 44, 41–58.

Ursell, F., 1978. On the exterior problems of acoustics: II. Mathematical Proceedings of Cambridge Philosophical Society 84, 545–548.